Cancer Research

Chimeric PD-1:28 Receptor Upgrades Low-Avidity T cells and Restores Effector Function of Tumor-Infiltrating Lymphocytes for Adoptive Cell Therapy

Ramona Schlenker[1], Luis Felipe Olguín-Contreras[1,2], Matthias Leisegang[3,4], Julia Schnappinger[1,2], Anja Disovic[1,2], Svenja Rühland[5,6], Peter J. Nelson[5], Heinrich Leonhardt[6], Hartmann Harz[6], Susanne Wilde[7], Dolores J. Schendel[7], Wolfgang Uckert[8,9], Gerald Willimsky[3,10], and Elfriede Noessner[1,2]

Abstract

Inherent intermediate- to low-affinity T-cell receptors (TCR) that develop during the natural course of immune responses may not allow sufficient activation for tumor elimination, making the majority of T cells suboptimal for adoptive T-cell therapy (ATT). TCR affinity enhancement has been implemented to provide stronger T-cell activity but carries the risk of creating undesired cross-reactivity leading to potential serious adverse effects in clinical application. We demonstrate here that engineering of low-avidity T cells recognizing a naturally processed and presented tumor-associated antigen with a chimeric PD-1:28 receptor increases effector function to levels seen with high-avidity T cells of identical specificity. Upgrading the function of low-avidity T cells without changing the TCR affinity will allow a large arsenal of low-avidity T cells previously thought to be therapeutically inef-

ficient to be considered for ATT. PD-1:28 engineering reinstated Th1 function in tumor-infiltrating lymphocytes that had been functionally disabled in the human renal cell carcinoma environment without unleashing undesired Th2 cytokines or IL10. Involved mechanisms may be correlated to restoration of ERK and AKT signaling pathways. In mouse tumor models of ATT, PD-1:28 engineering enabled low-avidity T cells to proliferate stronger and prevented PD-L1 upregulation and Th2 polarization in the tumor milieu. Engineered T cells combined with checkpoint blockade secreted significantly more IFNγ compared with T cells without PD-1:28, suggesting a beneficial combination with checkpoint blockade therapy or other therapeutic strategies. Altogether, the supportive effects of PD-1:28 engineering on T-cell function make it an attractive tool for ATT. *Cancer Res; 77(13); 3577–90. ©2017 AACR.*

Introduction

Magnitude, quality, and functional polarization of an immune response are crucial for the control of many diseases, including cancer. Examples of successful implementation of these principles are the adoptive transfer of selected highly tumor-reactive T cells

(1) and checkpoint inhibition (2), which achieve remarkable tumor regressions even in patients who have failed previous treatments. Despite these successes, immunotherapeutic concepts need to be improved as no or low response is still a frequent outcome. Although there is consensus that durable antitumor responses require highly active T cells, it is not clear how this is best achieved. At least two major impediments have been identified that impinge upon achieving this prerequisite: inherent intermediate- to low-affinity T-cell receptors (TCR) of antitumor T cells that may not mount a successful tumor-specific response (3, 4), and functional inactivation of T in the tumor milieu (5–8).

Experimentally generated high-affinity TCRs might be advantageous by boosting effector function and proliferation, thereby persisting longer and in larger numbers as compared with T cells with low-affinity TCRs, but they may also bear an increased risk of unwanted toxicities (3, 4, 9–12). Low-avidity T cells would gain value if their effector functions could be enhanced, as they are reported to be less susceptible to tolerization and may represent a lower toxicity risk (3, 4, 13, 14).

Loss of function following tumor infiltration occurs independently of T-cell avidity (5–8). Thus, preventing or delaying functional loss and endowing reactive T cells with the capacity to maintain antitumor effector functions longer in the tumor environment are imperatives for achieving more effective T-cell response. Functional inactivation may occur due to blockade of

AACR 3577

Schlenker et al.

TCR signaling, loss of cytotoxic proteins, lack of persistence, and functional polarization from an antitumor Th1 to a less favorable Th2 phenotype (15–21).

To overcome these activation restrictions, we focused on costimulation and coinhibition signals controlling strength and duration of the T-cell response (22). In challenging environments, costimulation has been shown to improve effector function as it enables refill of lytic granules and T-cell expansion (23, 24). Thus, we generated chimeric receptors composed of the PD-1 extracellular domain and the CD28 signaling domain (PD-1:28) following published designs (25, 26). PD-1:28–engineered T cells should receive costimulatory signals to support survival, proliferation, and TCR signaling when interacting with PD-1 ligand (PD-L1) on tumor cells. Simultaneously, coinhibitory interaction with expressed native PD-1 should be opposed, ameliorating another major hurdle of efficient antitumor function in PD-L1[+] tumor milieus. All this will occur without changing the TCR specificity.

Here, we demonstrate that PD-1:28 chimeric receptors upgrade low-avidity T cells and restore effector function of tumor-suppressed human tumor-infiltrating lymphocytes (TIL). Through PD-1:28 signaling, T cells receive support in processes essential for tumor growth control, that is, stronger proliferation in solid tumor milieus and prevention of Th2 polarization. Moreover, PD-1:28–facilitated T-cell support seems to work synergistic with anti-PD-L1 checkpoint blockade, suggesting that PD-1:28 engineering of T cells can be beneficially combined with checkpoint blockade and potentially other immunotherapies.

Materials and Methods

Cell lines, PBMCs, and TILs

Cell lines were grown in RPMI1640/1% L-glutamine/1% nonessential amino acids/1% sodium pyruvate/1% penicillin/streptomycin (RPMI basic), and 12% FCS at 37°C/6.5% CO_2. Cell lines were kept in continuous culture for no longer than 2 months. Mycoplasma testing was performed monthly using VenorGeM Classic (Minerva Biolabs). All cell lines were authenticated by flow cytometry to express the relevant molecules, HLA-A2, tyrosinase or TCR53 antigen, without or with PD-L1, as required (see Results). The following cell lines were used: HEK293 cells (positive for HLA-A2, negative for endogenous PD-L1 by flow cytometry, obtained from H. Engelmann, Institute of Immunology, Munich, Germany, in 1997) were transduced in our laboratory to express tyrosinase (HEK/Tyr) or tyrosinase and PD-L1 (HEK/Tyr/PD-L1). Single-cell clones were selected for comparable HLA-A2 and tyrosinase expression (see Results); human melanoma lines: SK-Mel23 (ATCC HTB71, obtained from M.C. Panelli in 2001, NIH, Bethesda, MD), FM3, FM55, FM86 (obtained from P. thor Straten in 2014, Danish Cancer Society, Copenhagen, Denmark), WM115 (ESTDAB-066), WM266.4A (ESTDAB-076; both purchased in 2003); human nonmelanoma lines: renal cell cancer RCC-53 and RCC-26 (generated in our laboratory in 1993 and 1991, respectively), squamous cell carcinoma UT-SCC-15 and glioblastoma U-373 (obtained from co-author P.J. Nelson in 2002; ref. 27). Murine mastocytoma line P815 (ATCC TIB-64, purchased in 1995) was authenticated by morphology and expression of FcγR, which is required for antibody coating.

Murine hepatocellular carcinoma (HCC) line 434 originated in LoxP-TAg mice (28) and was grown in RPMI-basic/12% FCS/0.05% β-mercaptoethanol (mouse medium). Authentication was done by testing SV40LT, H2-D[b], and PD-L1 expression.

Human peripheral blood mononuclear cells (PBMC) were from healthy donors (HD). Transduced T cells were grown in RPMI-basic/10% human serum (T-cell medium) and 50 U/mL IL2, or as indicated. TILs were tissue suspensions prepared from postsurgery clear cell renal cell carcinoma (ccRCC) as described previously (16). Detailed pathologic features are described in Supplemental Material. Blood and tissues were collected with donors' and patients' informed consent in accordance with the Declaration of Helsinki and after approval by the Institutional Review Board of Ludwig-Maximilian University (Munich, Germany).

Constructs, expression vectors, electroporation, and retroviral transduction

pMP71 plasmids encoding TCR-T58, TCR-D115 (both tyrosinase-epitope(AA$_{366-377}$)-specific/HLA-A2-restricted), and TCR53 have been described previously (27). Various costimulatory chimeric receptors were designed on the basis of the extracellular domain (ECD) of PD-1 and the intracellular domain (ICD) of CD28 containing the signaling motifs YMNM, PRRP, and PYAP (Fig. 1A). The chimeric sequence PD-1:8^{tm}:28 was composed of PD-1 ECD (AA1-170), CD8α (AA128-210) as linker and transmembrane domain (TMD), followed by CD28 ICD (AA180-220). PD-1:cys28^{tm} contains PD-1 ECD (AA1-155) followed by CD28 TMD-ICD (AA141-220), which includes the membrane-proximal cysteine residue at position AA141 (adapted from Prosser and colleagues; ref. 26). PD-1:28^{tm} contains PD-1 ECD (AA1-165) followed by CD28 TMD-ICD (AA153-220) omitting the extracellular portion with the cysteine (adapted from Ankri and colleagues; ref. 25). PD-1trunc is a truncated PD-1 sequence (AA1-201; ref. 25). Murine mPD-1:28^{tm} contains murine PD-1 ECD (AA1-169) and murine CD28 TMD-ICD (AA151-218). Chimeric sequences were ordered from GeneArt.

Chimeric receptors were expressed in human T cells either by electroporation with in vitro–transcribed RNA cloned in pGEM vector (provided by S. Milosevic, Medigene GmbH) or by retroviral transduction using the pMP71 vector as described previously (29). Murine splenocytes were retrovirally transduced as described previously (29). For experimental details, see Supplementary Material.

Human melanoma xenograft and murine HCC models

The animal experiments were performed according to and with approval of the Landesamt für Gesundheit und Soziales, Berlin, Germany (HCC model) or they were approved by the Regierung von Oberbayern, Germany and performed in accordance with the Animal Care and Use Committee at the Helmholtz Zentrum München (NSG model).

For the xenograft model, NSG mice (Charles River Laboratories; 7–11 weeks old) were injected subcutaneously with 5×10^6 SK-Mel23 cells. Grown to approximately 800 mm^3 (15–20 days), tumors were injected intratumorally with 6×10^6 carboxyfluorescein diacetate succinimidyl ester (CFSE)-labeled T cells. Tumors were harvested and weighed 4 hours, 1, 2, 4, 6, and 10 days after adoptive T-cell therapy (ATT). Single-cell suspensions were prepared for flow cytometry as described previously (16). Tumors were measured using a caliper prior to T-cell injection and before mice were sacrificed. Tumor volumes were calculated using the formula; volume = (length × width^2) × 0.52. For Matrigel plug
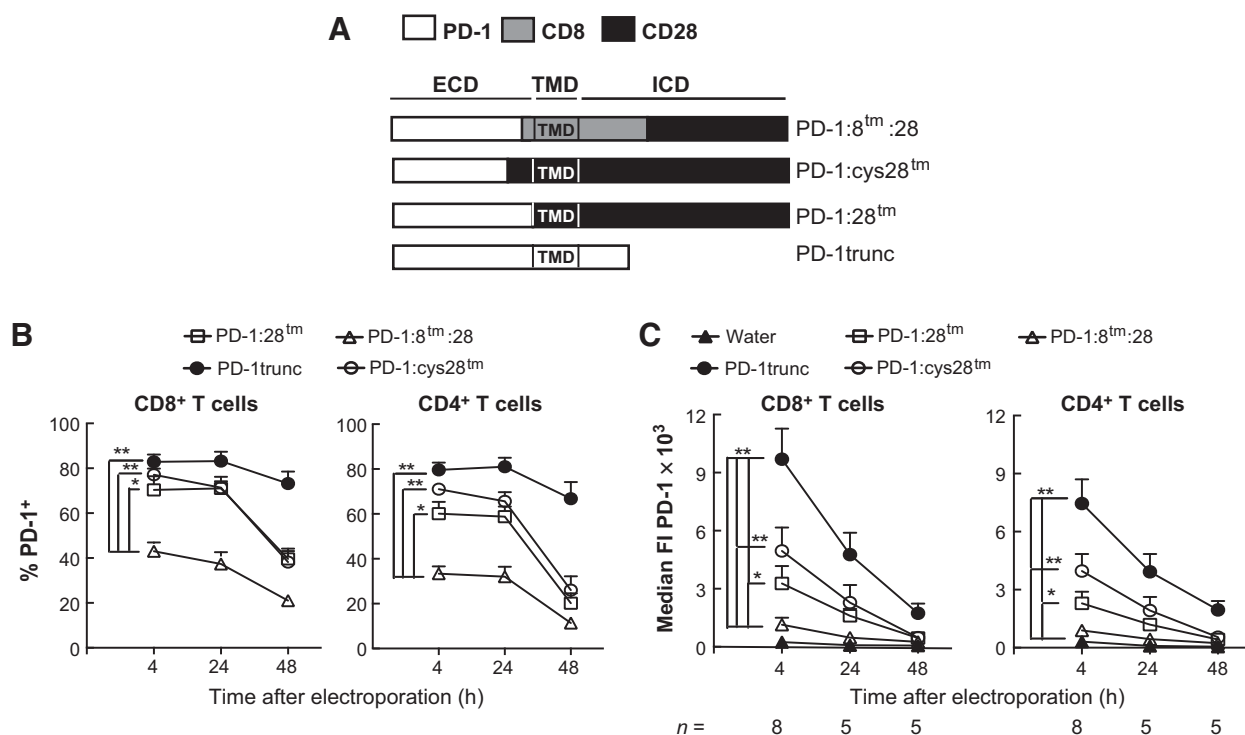
Figure 1.
PD-1:28 chimeric receptor expression is dependent on the origin of the transmembrane domain. **A,** Design of chimeric costimulatory receptors. White regions represent domains derived from PD-1, gray and black regions are derived from CD8 and CD28, respectively. **B** and **C,** Expression of chimeric receptors 4, 24, and 48 hours after *in vitro*–transcribed RNA electroporation among CD8^{+} and CD4^{+} T cells determined by flow cytometry staining of PD-1. Shown are mean values (+SEM) of indicated number of experiments for % PD-1^{+} cells (**B**) and median FI of PD-1. **C,** Statistics, Wilcoxon matched-pairs signed rank test, *, $P < 0.05$; **, $P < 0.01$.

assays, SK-Mel23 (HLA-A2[+]Tyr[+]) and HEK293 (HLA-A2[+]Tyr[-]) were labeled with CellTracker Deep Red fluorescent dye (1.5 μmol/L, Thermo Fisher Scientific) or Vybrant CFDA-SE Cell Tracer Kit (1.5 μmol/L, Invitrogen), respectively, and both additionally labeled with 2 μmol/L PKH26 (Sigma-Aldrich). SK-Mel23, HEK293 (each 2×10^6), and T cells (4×10^6) in 150 μL PBS were mixed with 200 μL Matrigel (Corning) and injected subcutaneously into NSG mice. IL15 (300 U) was given intraperitoneally. Plugs were recovered after 2 days and single-cell suspension prepared for flow cytometry. CFSE-(HEK293) and Deep Red–positive cell (SK-Mel23) percentages were determined among gated PKH26^{+}/CD45^{-} cells. Specific killing was calculated using the formula:
$$\% \text{ Specific killing} = [1 - (\text{ctrl}\tfrac{\%SK-Mel23}{\%HEK293})/(\text{sample}\tfrac{\%SK-Mel23}{\%HEK293})] \times 100,$$
whereby ctrl is cell mixture without T cells and sample is cell mixture with T cells.

The HCC mouse model has been described previously (ref. 28, and Supplementary Material). The ATT experiment was performed as outlined in the results and detailed in Supplementary Material.

Multiparameter flow cytometry and FACS sorting of TILs

Flow cytometry was performed with LSRII (BD Biosciences) and FlowJo 8.8.7 software. PD-1:28 chimeric receptor and transgenic TCRs (TCR-T58, TCR-D115) expression was analyzed using anti-PD-1-APC (eBioscience), anti-mouse TCRβ-constant region (mTCR)-PB (BioLegend), anti-CD3-PE-Cy7 (BioLegend), anti-CD4-APC-A780 (eBioscience), anti-CD8-V500 (BD), anti-Ki-67-Alexa-Fluor-700 (BioLegend), anti-PD-L1-BV421 (BD Biosciences), and 7-AAD (Sigma-Aldrich). Absolute cell numbers of intratumoral T cells were determined using Flow-Count Fluorospheres (Beckman Coulter). HEK293 and tumor lines were analyzed using anti-HLA-A2 (ATCC HB54) plus anti-mouse IgG1-A488 (Invitrogen), anti-PD-L1-FITC (BD Biosciences), anti-tyrosinase (Upstate Biotechnology) plus anti-mouse IgG2a-A647 (Invitrogen), and 7-AAD. T cells were stimulated with HEK/Tyr/PD-L1 cells at 1:2 (30 minutes/37°C), then stained with anti-CD45-PE-Cy7 (BioLegend), anti-CD8-V500, anti-pERK (pT202/pY204; Cell Signaling Technology) plus anti-rabbit IgG-A647 (Invitrogen) or anti-pRPS6 (pS235/pS236)-A647 (Cell Signaling Technology), and 7-AAD. Cells were fixed using Phosflow Cytofix Buffer (BD Biosciences) and permeabilized with Phosflow Perm Buffer III (BD Biosciences).

T cells from NSG xenograft tumors were analyzed using anti-CD45-PE-Cy7, anti-CD8-PB (BD Biosciences), anti-PD-1-APC, and 7-AAD. TILs and splenocytes from mice HCC tumors were stained using anti-CD3-APC-Cy7 (BioLegend), anti-CD19-V450 (eBioscience), anti-CD45-PE-Cy7 (eBioscience), anti-PD-1-PerCP-Cy5.5 (BioLegend), anti-Thy1.1-A647 (BioLegend), and propidium iodide (Sigma-Aldrich).

Tumor suspensions from ccRCC were stained with anti-CD45-PE-Cy7, anti-CD3-PB (both BioLegend), anti-CD11c-APC, and near-IR fluorescence-reactive viability dye (Invitrogen) and sorted as CD45^{+}/live/single/CD3^{+}/CD11c^{-}/small lymphocytes (FACS Aria IIIu, BD Biosciences).

Schlenker et al.

Cocultures and cytokine assays

T cells were stimulated with HEK/Tyr or HEK/Tyr/PD-L1 at 1:2 with or without antibodies blocking PD-1/PD-L1 (20 μg/mL, BioLegend). Human TILs and PBMCs were stimulated at 1:1 with OKT3/PD-L1-Fc (R&D Systems)–loaded P815 cells (each $5 \mu g/1 \times 10^6$ cells). Murine TILs and splenocytes were stimulated with HCC434 or PMA/I (50/500 ng/mL; Sigma-Aldrich). Supernatants were harvested after 16 hours and analyzed by ELISA (BD Biosciences) or Bio-Plex (Bio-Rad). Cytokine levels were normalized to the percentage of $mTCR^+CD8^+$ T cells.

Tumor spheroids and microscopic imaging

Spheroids were generated by seeding 800 SK-Mel23 cells into hanging drops. On day 3, single spheroids were confronted with 1.5×10^4 T cells labeled with CMFDA (Thermo Fisher Scientific) for 30 minutes. Nonattached T cells were removed and T cells/spheroids incubated in hanging drops with CellEvent Caspase-3/7 Red Detection Reagent (Thermo Fisher Scientific) for 24 hours followed by fixation. Samples were imaged up to a depth of 70 μm using a spinning disk confocal Nikon TiE microscope. Invaded $CMFDA^+$ T cells and CellEvent Caspase-3/7–positive apoptotic cells were counted using Fiji software (see Supplementary Material for details).

Chromium release assay

Chromium release assay was performed as described previously (16).

Statistical analysis

Statistical tests, indicated in figure legends, were performed using GraphPad Prism 6 software.

Results

PD-1:28 chimeric receptor expression depends on the origin of the transmembrane domain

To facilitate costimulation of T cells in tumor environments, we designed costimulatory chimeric receptors encompassing the ECD of PD-1 and the ICD of CD28. Different receptor designs (Fig. 1A) were compared regarding surface expression and effect on T-cell function: (i) PD-1:8^{tm}:28; (ii) PD-1:cys28^{tm}; (iii) PD-1:28^{tm}; and (iv) truncated PD-1 (PD-1trunc) without signaling capacity.

Human activated T cells were electroporated with *in vitro*–transcribed RNA encoding the various receptors. Four, 24, and 48 hours later, surface expression of the receptors on $CD3^+CD8^+$ and $CD3^+CD4^+$ T cells was analyzed by flow cytometry. Four hours after electroporation, the PD-1trunc receptor was best expressed in terms of percentage of $PD-1^+$ cells and median fluorescence intensity (median FI; Fig. 1B and C). Percentages of PD-1 surface–positive cells were not significantly different between PD-1trunc and either PD-1:cys28^{tm} or PD-1:28^{tm} at 4 and 24 hours after electroporation. However, median FI was significantly higher for T cells expressing PD-1trunc compared with PD-1:cys28^{tm} or PD-1:28^{tm}. PD-1:8^{tm}:28 showed significantly lower surface expression compared with PD-1trunc, PD-1:cys28^{tm}, and PD-1:28^{tm} regarding percentage of positive cells and levels of surface expression.

PD-1:cys28^{tm} and PD-1:28^{tm} augment T-cell cytokine secretion and signaling

Effects of chimeric receptors on T-cell function were analyzed by assessing TCR-induced cytokine secretion. Human T cells were transduced to stably express one of two different HLA-A2–restrict-ed tyrosinase-specific TCR, T58 or D115, followed by transient expression of chimeric costimulatory receptor (Fig. 2A). These T cells were stimulated with $HLA-A2^+$ HEK293 cells expressing either the target antigen tyrosinase (HEK/Tyr) alone or together with PD-L1, the ligand for PD-1 (HEK/Tyr/PD-L1; Fig. 2B). Despite artificial expression of tyrosinase, HEK/Tyr cells were low activators of TCR-T58- or TCR-D115-T cells stimulating less IFNγ secretion and lower cytotoxicity than the natural tumor target SK-Mel23 (Fig. 2C–E). The HEK-cell system was further used as it allowed assessing the contribution of PD-L1 interacting with PD-1:28 chimeric receptors to T-cell function.

TCR-T58- and TCR-D115–expressing T cells with PD-1:28^{tm} or PD-1:cys28^{tm} secreted significantly more IL2 and IFNγ when stimulated with HEK/Tyr/PD-L1 compared with HEK/Tyr cells (Fig. 3A). The PD-1:8^{tm}:28 chimeric receptor had no effect on IL2 and IFNγ production of T cells expressing either transgenic TCR. Expression of PD-1trunc did not alter cytokine secretion of TCR-T58-T cells, but increased cytokine secretion of TCR-D115-T cells when stimulated with HEK/Tyr/PD-L1 cells, indicating that the truncated PD-1 is not an inert construct. The effect is likely due to competitive attenuation of negative signals through T cell–upregulated native PD-1 interacting with PD-L1 on target cells. Therefore, T cells electroporated with water (control) must be the reference for experiments assessing PD-1:28 effects.

To demonstrate that improved function was due to specific ligand receptor binding, blocking antibodies to PD-1 and PD-L1 were added to cocultures. No effect was seen in cocultures of untransfected T cells with HEK/Tyr or HEK/Tyr/PD-L1 cells. Similarly, no effect was seen when PD-1:28^{tm} T cells were cocultured with HEK/Tyr cells. However, when blocking antibodies were added to cocultures of PD-1:28^{tm} T cells with HEK/Tyr/PD-L1 cells, cytokine levels were reduced to those in HEK/Tyr cocultures, thus representing the levels induced by the TCR alone (Fig. 3B).

The molecular basis for the significant increase in cytokine secretion upon stimulation through PD-1:28^{tm} was investigated by assessing phosphorylation of MAP kinase ERK and ribosomal protein S6 (RPS6) using phospho-flow cytometry. After stimulation with HEK/Tyr/PD-L1, phosphorylation of ERK was enhanced 4.4-fold in PD-1:28^{tm}–engineered T cells compared with water control. Regarding pRPS6, 43% of PD-1:28^{tm} T cells were positive for the phosphorylated form compared with 33% in control (Fig. 3C and D). Although these differences were not significant, there was a clear and reproducible trend toward increased phosphorylation of both ERK and RPS6 when T cells received dual stimulation through PD-1:28^{tm} and their TCRs.

PD-1:cys28^{tm} and PD-1:28^{tm} upgrade low-avidity T cells to achieve cytokine secretion comparable with high-avidity T cells

Next, we assessed whether PD-1:28 engineering could improve functional responses of T cells with low-avidity TCRs recognizing tumor-expressed self-antigens.

T58 and D115 are high- and low-avidity TCRs, respectively, that recognize the same HLA-A0201–restricted tyrosinase epitope. Low-avidity TCR-D115–expressing T cells secreted significantly less IL2 and IFNγ than T cells expressing TCR-T58 when stimulated with HEK/Tyr/PD-L1 target cells (Fig. 4A). TCR-D115-transgenic T cells coexpressing PD-1:28^{tm} or PD-1:cys28^{tm} showed augmented cytokine secretion that reached levels comparable with high-avidity TCR-T58–transduced T cells stimulated with $PD-L1^+$ target cells. Thus, activation of the costimulatory cascade
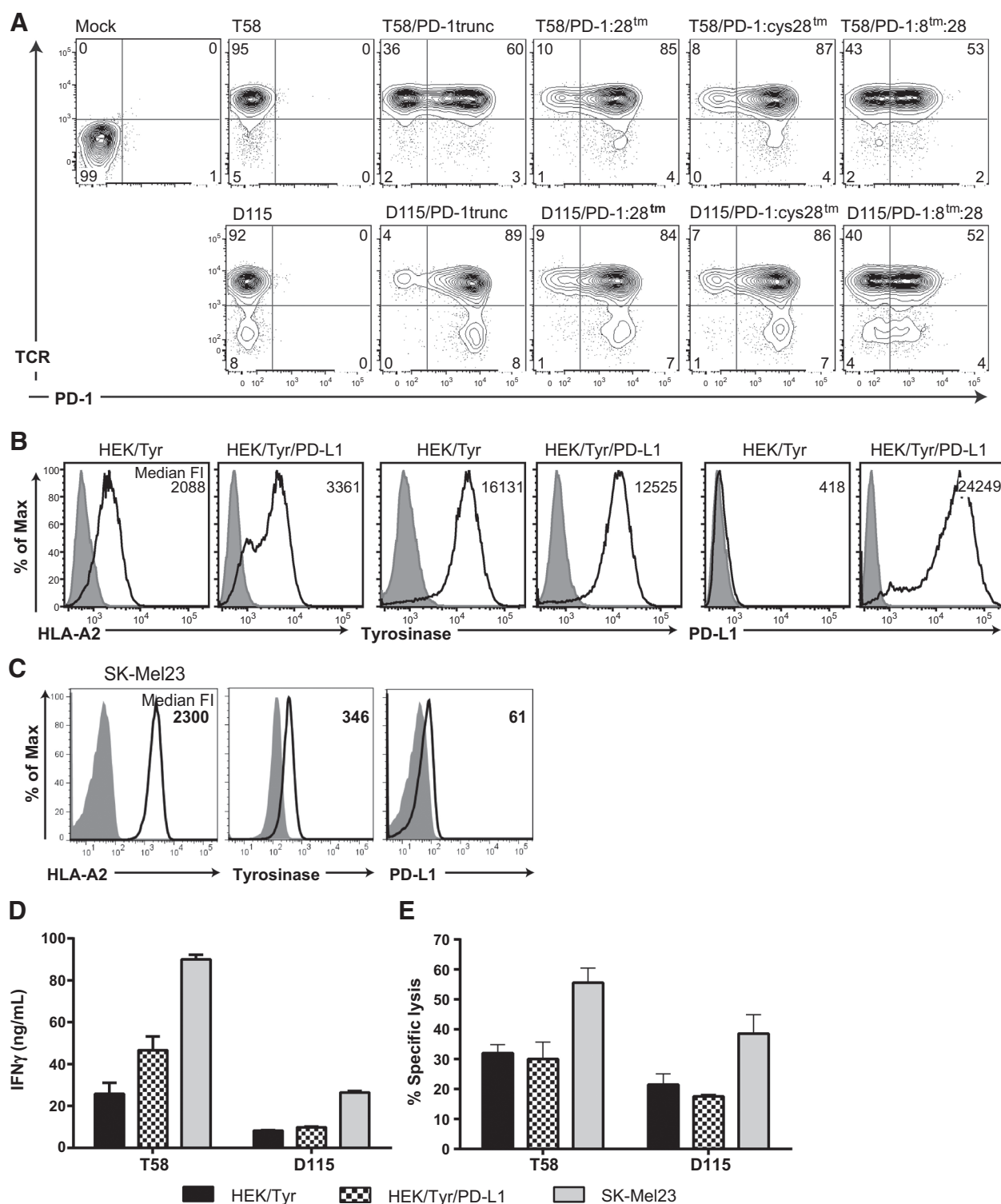
Figure 2.
Human TCR-T58- and TCR-D115-T cells, HEK293/Tyr/PD-L1, melanoma target cell lines. **A,** Human T cells were retrovirally transduced with the tyrosinase-specific TCRs, T58 or D115, and electroporated with *in vitro*–transcribed RNA coding for the chimeric receptors. Dot plots showing TCR and chimeric receptor expression in CD8^{+} T cells. **B** and **C,** Histograms showing HLA-A2, tyrosinase, and PD-L1 expression in HEK/Tyr, HEK/Tyr/PD-L1 (**B**), and SK-Mel23 (**C**) cells. Black line histograms, specific antibody staining; gray filled histograms, control staining. Numbers are median FI of indicated marker. **D** and **E,** IFNγ secretion and cytotoxicity of human TCR-T58- and TCR-D115-T cells. TCR-T58- and TCR-D115-T cells were cocultured with either HEK/Tyr, HEK/Tyr/PD-L1, or SK-MEL23 at effector-to-target cell ratio of 1:2 for 16 hours; then, IFNγ was measured in supernatants (**D**) or T cells were cocultured with [51]chromium-labeled targets at an effector-to-target ratio of 6:1 for 4 hours (**E**).

Schlenker et al.
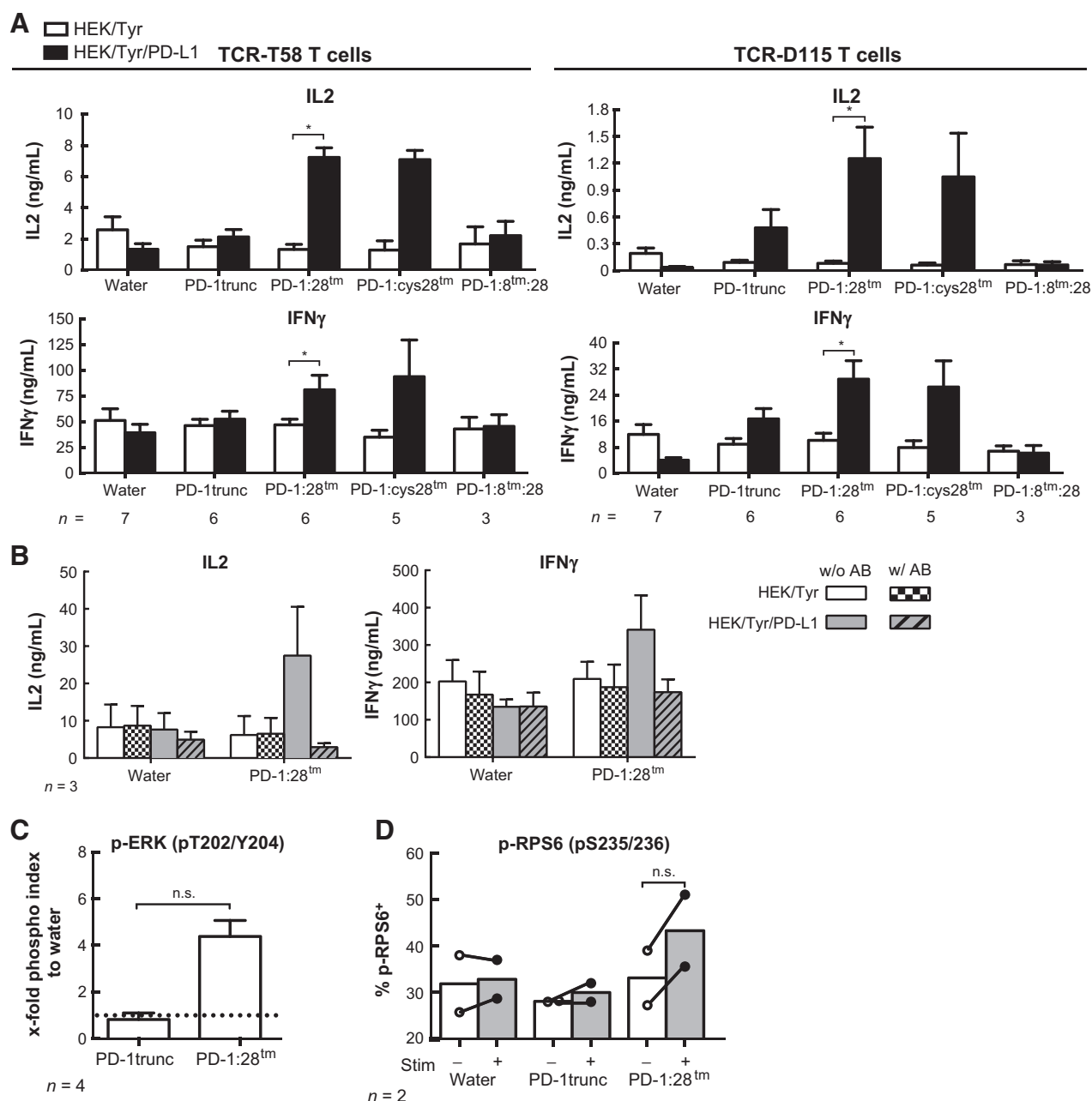
Figure 3.
PD-1:cys28[tm] and PD-1:28[tm] augment T-cell cytokine secretion and signaling. **A,** TCR-T58- or TCR-D115–transduced and chimeric receptor–electroporated T cells were stimulated with HEK/Tyr cells and HEK/Tyr/PD-L1. Coculture supernatants were harvested after 16 hours and analyzed for cytokine content. Depicted is the amount of IL2 and IFNγ secreted by 25,000 CD8^{+}mTCR^{+} T cells [mean of indicated number (n) of experiments + SEM]. Wilcoxon matched-pairs signed rank test. *, $P < 0.05$. **B,** TCR-T58–transduced and chimeric receptor–electroporated T cells were stimulated with HEK/Tyr or HEK/Tyr/PD-L1 cells with (w) or without (w/o) blocking antibodies (AB) to PD-1 and PD-L1. Coculture supernatants were harvested after 16 hours and analyzed for IL2 and IFNγ content. Depicted is the amount of cytokines secreted by 25,000 CD8^{+}mTCR^{+} T cells (mean + SEM, $n = 3$). **C** and **D,** TCR-T58–transduced and chimeric receptor–electroporated T cells were stimulated with HEK/Tyr/PD-L1 cells, and phosphorylation of ERK and RPS6 was analyzed by phospho-flow cytometry. Regarding ERK phosphorylation (**C**), the phospho index is depicted as x-fold change between chimeric receptor–electroporated and water-electroporated CD8^{+} T cells. ERK phospho-index is the percentage of p-ERK^{+} cells multiplied by the median FI of p-ERK^{+} cells (mean + SEM, $n = 4$). Regarding RPS6 phosphorylation (**D**), the percentage of p-RPS6^{+}CD8^{+} T cells in unstimulated (white bars) and stimulated (gray bars) cells is depicted (mean, $n = 2$). n.s., nonsignificant.

through PD-1:28 chimeric receptor allowed cells with a low-avidity TCR to approximate the cytokine function of cells with a high-avidity TCR. Similar results were observed for cytotoxicity

(Fig. 4B). Low-avidity TCR-D115/Mock T cells showed lower specific lysis of HEK/Tyr and HEK/Tyr/PD-L1 target cells than the high-avidity TCR-T58/Mock T cells. PD-1:28[tm] expression in

TCR-D115-T cells increased cytotoxicity against PD-L1$^+$ HEK/Tyr cells reaching levels equal to TCR-T58-T cells, while the cytotoxicity against PD-L1$^-$ HEK/Tyr was unchanged.

PD-1:28^{tm} engineering not only enhanced T-cell response against HEK/Tyr/PD-L1 cells but also enabled T cells to respond stronger to tumor lines with endogenous expression of antigens and PD-L1. The extent of functional improvement followed the level of PD-L1 surface expression on the tumor cells. Melanoma lines grown in standard culture exhibited low PD-L1 surface expression (FI range, 180–540) and PD-1:28^{tm}-engineered TCR-D115-T cells reached on average 1.4-fold (range, 1.3- to 1.6-fold change) higher IFNγ and IL2 secretion compared with TCR-D115-T cells without PD-1:28^{tm} (Fig. 4C, and data not shown). PD-L1 was strongly induced on SK-Mel23 grown as 3D spheroids, and significantly higher T-cell numbers and more apoptotic tumor cells were recovered from spheroids cocultured with PD-1:28^{tm}–engineered TCR-D115-T cells compared with TCR-D115-T cells without PD-1:28^{tm} (Fig. 4D). Higher PD-L1 levels were also seen on nonmelanoma lines (FI range, 850–1830) that express the natural tumor antigen recognized by TCR53 (27). Consistent with the PD-L1 expression on TCR53 target cells, TCR53-T cells derived strong benefit from PD-1:28^{tm} engineering with 1.4- to 2.5-fold improvement of IFNγ secretion (Fig. 4E). These results indicate that T cells will benefit more from PD-1:28^{tm} engineering in tumor milieus where PD-L1 is highly expressed.

PD-1:28^{tm} can reinstate function in unresponsive tumor-infiltrating T lymphocytes from human RCC and can work in synergy with checkpoint blockade therapy

We previously demonstrated that TILs from human RCC tissue show deficits in degranulation and IFNγ secretion, in part due to insufficient activation of signaling molecules AKT, ERK, and JNK (16). As CD28 costimulation fosters activation of intracellular signaling molecules, including AKT, ERK, and JNK, we sought to determine whether costimulation through PD-1:28^{tm} could restore functionality in unresponsive TILs. Therefore, sorted CD3$^+$ TILs from RCC tissues were electroporated with PD-1:28^{tm} or water and stimulated with target cells (P815 loaded with anti-CD3/PD-L1-Fc). CD3$^+$ TILs electroporated with water did not secrete IFNγ upon stimulation, while CD3$^+$ TILs electroporated with PD-1:28^{tm} clearly produced IFNγ at levels comparable with PBMCs of HD (Fig. 5A). Similar improvement was observed for IL2 secretion (Fig. 5B). As TILs in the tumor microenvironment can be polarized toward Th2 or regulatory IL10 programs, we addressed the question whether facilitated costimulation through PD-1:28 might unleash undesirable Th2 or IL10 cytokines. However, neither mock-transfected nor PD-1:28^{tm}–transfected TILs (n = 3) secreted detectable levels of IL4, IL5, IL13, or IL10 (data not shown). These cytokines were detected at low levels in supernatants of one (IL4) and two (IL13) HD-PBMCs, yet levels were not augmented when costimulated through PD-1:28^{tm}. TNF levels in supernatants of TILs were very low and marginally increased after facilitated costimulation. HD-PBMCs secreted detectable amounts of TNFα; yet, levels did not change with PD-1:28^{tm} costimulation (data not shown). Thus, costimulation through PD-1:28^{tm} can reinstate functionality in TILs that had lost activity in the tumor microenvironment. Costimulation through PD-1:28^{tm} rescued Th1 cytokine secretion (IFNγ, IL2), while TNFα, Th2 cytokines, or IL10 were not affected.

Presumably, ATT will be combined with checkpoint blockade using anti-PD-1 or anti-PD-L1 antibodies. To explore whether PD-1:28^{tm}-engineered T cells would benefit in this situation, we added titrated concentrations of anti-PD-L1 antibody to cocultures of TCR-D115/Mock or TCR-D115/PD-1:28^{tm} T cells with HEK/Tyr or HEK/Tyr/PD-L1 and measured secreted IFNγ. Anti-PD-L1 antibody did not change IFN-γ levels if the target cell was negative for PD-L1 (Fig. 5C). If the target expressed PD-L1 and the T cell had no PD-1:28^{tm}, IFNγ levels increased with raising anti-PD-L1 antibody concentration, presumably due to interrogating negative signals mediated through endogenously upregulated PD-1. Of note, in cocultures of PD-L1$^+$ target cells with PD-1:28^{tm} T cells, low concentrations of anti-PD-L1 antibody strongly augmented IFNγ while high antibody concentration prevented this induction. PD-1:28^{tm}-engineered T cells combined with checkpoint blockade secreted significantly more IFNγ compared with T cells without PD-1:28^{tm}, indicating that PD-1:28^{tm} T-cell engineering can work in synergy with checkpoint blockade therapy.

PD-1:28^{tm} fosters intratumoral T-cell proliferation and enables better tumor control in a human melanoma xenograft model

Effects of PD-1:28^{tm} expression in T cells in vivo was studied using a human melanoma xenograft mouse model based on NSG mice carrying established vascularized subcutaneous melanoma tumors formed by the SK-Mel23 melanoma line (Fig. 6A). CFSE-labeled TCR-D115/Mock or TCR-D115/PD-1:28^{tm} T cells were injected intratumorally into tumors (802 mm^3 ± 83, mean ± SEM) and analyzed at 4 h, 1, 2, 4, 6 and 10 d after ATT by flow cytometry. It was observed that TCR-D115/Mock T cells stained positive for PD-1 on 1, 2, and 4 days after ATT. Thereafter, PD-1 staining decreased, but never completely disappeared (Fig. 6B and C). This temporary expression of endogenous PD-1 suggests that T-cell activation occurred within the tumor microenvironment, as PD-1 is expressed on recently activated T cells (30). Activation lasted until day 4 after ATT. For TCR-D115/PD-1:28^{tm} T cells, temporary expression of endogenous PD-1 could not be distinguished from the transgenic PD-1:28^{tm} expression. However, a temporary increase in median FI of PD-1 was observed with similar kinetics.

TCR-D115/PD-1:28^{tm} T cells lost CFSE intensity more rapidly and strongly than TCR-D115-T cells without PD-1:28^{tm} (Fig. 6D and E). The difference was significant at all time points (Fig. 6D), indicating that TCR-D115/PD-1:28^{tm} T cells responded faster and stronger to antigen-specific stimulation in the tumor microenvironment than TCR-D115 T cells without the chimeric costimulatory receptor. Survival could not be assessed in this model as T cells were injected into large tumors to ensure establishment of a challenging microenvironment. Animal regulatory restrictions did not allow extension of the observation time. However, compared over 7 days (Fig. 6F), tumors injected with TCR-D115/PD-1:28^{tm} T cells grew slower (median 1.5-fold increase) compared with tumors injected with TCR-D115 T cells without PD-1:28^{tm} (median 2.0-fold increase). While acknowledging the small sample size and absence of statistical significance, the data suggest that PD-1:28^{tm} costimulation can improve antitumor function of low-avidity T cells in the tumor milieu. Analysis of T cells recovered from 7-day tumors support this evidence: Higher T-cell numbers were found in tumors injected with TCR-D115/PD-1:28^{tm} T cells with higher percentages of Ki-67$^+$ cells and lower frequencies of T cells expressing PD-L1, compared with

Schlenker et al.
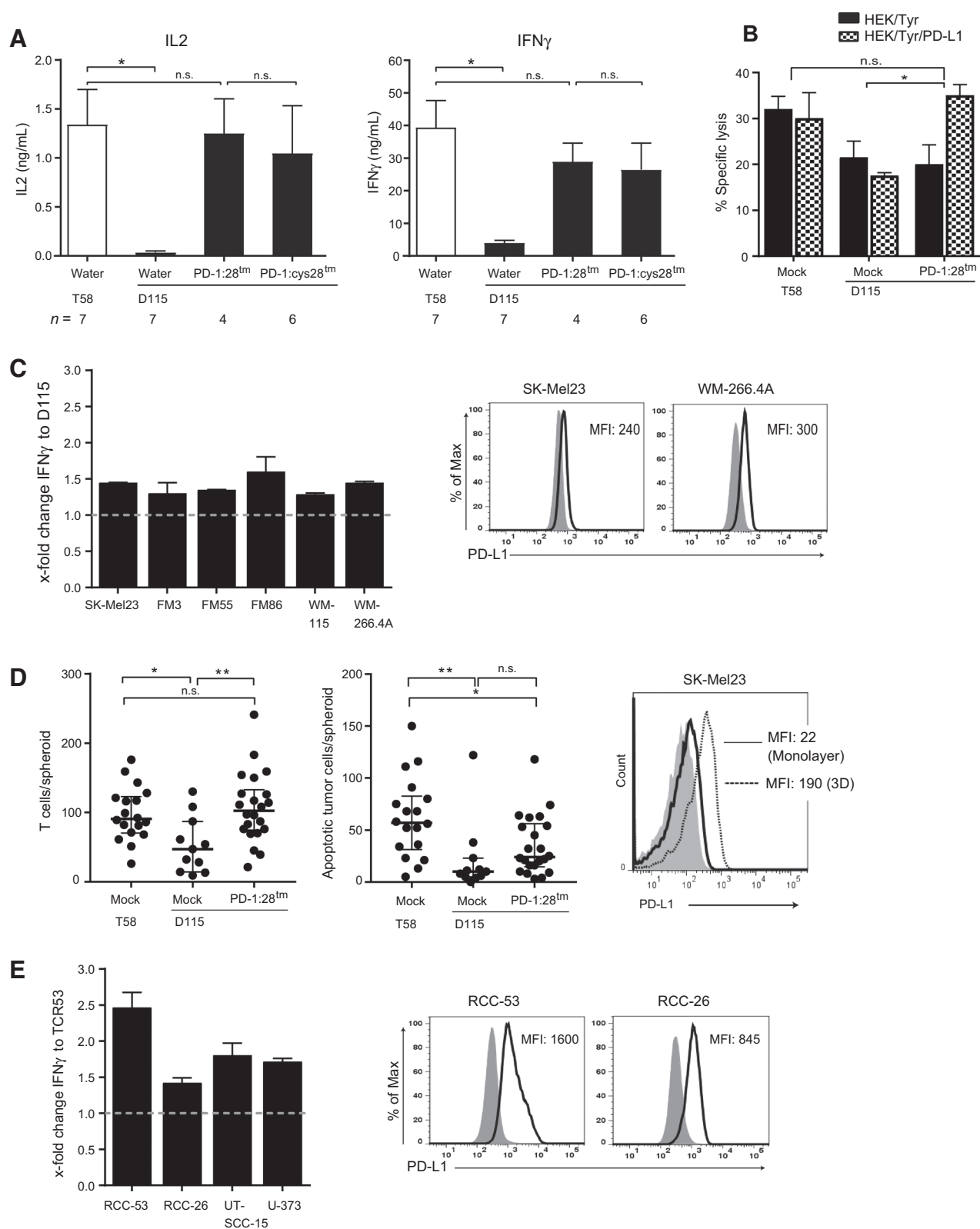
Figure 4.
PD-1:28 engineering upgrades low-avidity T cells and enhances T-cell activity against tumor cells. **A,** TCR-T58- or TCR-D115–transduced and chimeric receptor–electroporated T cells were stimulated with HEK/Tyr/PD-L1 cells. Coculture supernatants were harvested after 16 hours and analyzed for IL2 (left) and IFNγ (right). (Continued on the following page.)

Figure 5.
PD-1:28[tm] can reinstate Th1 response in dysfunctional TILs from human RCC and can synergize with anti-PD-L1 checkpoint inhibition. T cells were FACS-sorted from RCC tissue samples, electroporated with PD-1:28[tm] or water, and stimulated with anti-CD3 plus PD-L1/Fc-loaded P815 cells. PBMCs of HD were analyzed in parallel. Coculture supernatants were harvested after 16 hours and analyzed for IFNγ (ELISA; **A**) and IL2 (Bio-Plex; **B**). Each symbol corresponds to one patient or HD; lines connect T cells from the same individual ± PD-1:28[tm]. Bars are the mean + SEM. Mann–Whitney U test, *, $P < 0.05$. **C,** TCR-D115/Mock and TCR-D115/PD-1:28[tm] T cells were cocultured with HEK/Tyr and HEK/Tyr/PD-L1 at an effector-to-target ratio of 1:2 for 16 hours ± anti-PD-L1 antibody at indicated concentrations. Coculture supernatants were analyzed for IFNγ (ELISA). Depicted is the mean of two experiments + SD. Two-way ANOVA, *, $P < 0.05$; **, $P < 0.01$. n.s., nonsignificant.
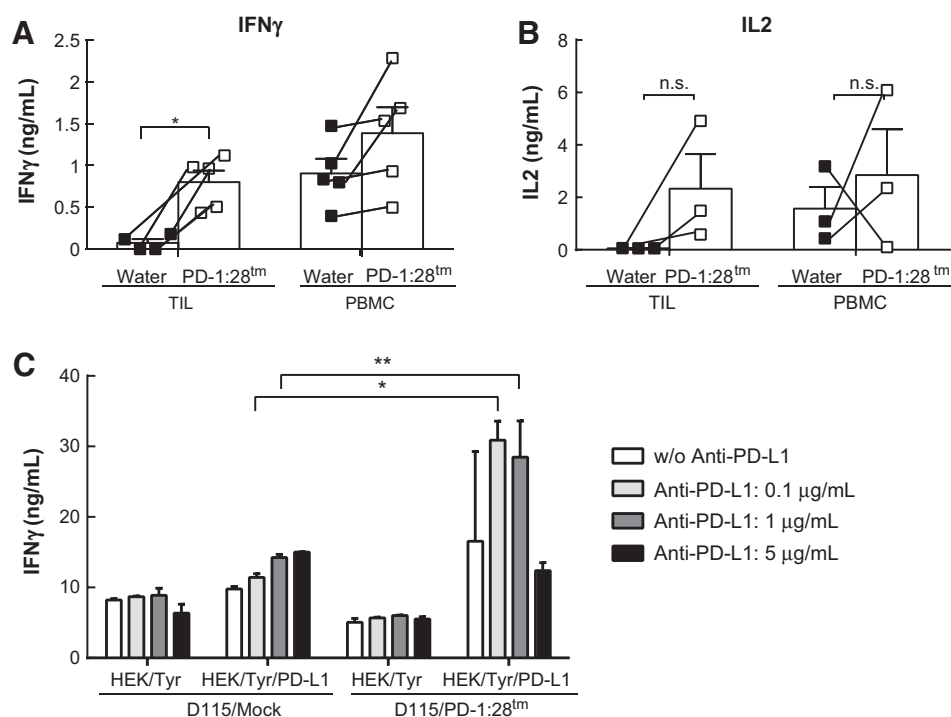
tumors injected with TCR-D115/Mock T cells (Fig. 6G). Higher T-cell numbers and better tumor control after ATT with TCR-D115/PD-1:28[tm] T cells are consistent with results from the spheroid model (Fig. 4D). Low T-cell numbers and high PD-L1 expression may explain the observed poorer tumor control through TCR-D115/Mock T cells, as PD-L1 on T cells has been described to inhibit T-cell expansion and function (31). Furthermore, in a Matrigel-killing assay in situ over 2 days (Fig. 6H), TCR-D115/PD-1:28[tm] T cells achieved on average 76.2% of SK-Mel23 killing, while killing through TCR-D115/MOCK T cells was much lower (59.3% on average).

PD-1:28[tm] shifts the cytokine balance of TILs in favor of antitumor Th1 cytokines in vivo

Limitations of NSG xenograft models led us to analyze the impact of PD-1:28[tm] chimeric receptors in a fully murine system. In the autochthonous HCC mouse model, T cells become exhausted after an initial phase of antitumor activity, and survival could be prolonged with anti-PD-L1 (28). To investigate whether PD-1:28[tm] could rescue exhausted T cells, splenocytes were isolated from mice 15 weeks after initiation of oncogenesis (it is assumed that T cells have lost control over tumor growth at this time point; ref. 28) and transduced with Thy1.1 to allow tracking after ATT,

alone or together with a murine PD-1:28[tm] (mPD-1:28[tm]). ATT was given to LoxP-TAg mice that carried occult tumors (week 12 after oncogene activation; Fig. 7B). Although ATT did not prolong survival (not shown), notable differences were observed in the TIL populations after ATT with T cells with or without mPD-1:28[tm]. Globally, there were no differences in percentages of CD3^{+} T cells or CD19^{+} B cells in tumors or spleens of mice with or without ATT (Fig. 7C and D). However, the cytokine profile of TILs in the PD-1:28[tm]-negative ATT was shifted toward Th2^{+}Th17 cytokines compared with splenocytes that were dominated by Th1 cytokines (Fig. 7E and F). PD-1 can inhibit Tc1/Th1 responses in the tumor microenvironment through SHP-2 (32) and, indeed, very high levels of PD-1 were observed among TILs (Fig. 7E, inset). Thus, endogenous PD-1 induction in the tumor microenvironment might contribute to the Th2 polarization of TILs. TILs from mice having received ATT with mPD-1:28[tm]-positive T cells had a more favorable Th1/Th2 balance with less Th2^{+}Th17 cytokines compared with TILs from mice given mPD-1:28[tm]-negative ATT, yet with a notable increase in IL10.

Discussion

Immunotherapy has emerged as a pillar of cancer therapy, although improvements are needed as response rates are still low

(Continued.) Depicted is the amount of cytokine secreted by 25,000 CD8^{+}mTCR^{+}T58^{+} or CD8^{+}mTCR^{+}D115^{+} T cells with or without PD-1:28 [mean of indicated number (n) of experiments + SEM]. Wilcoxon matched-pairs signed rank test, *, $P < 0.05$. n.s., nonsignificant. **B,** TCR-T58/Mock-, TCR-D115/Mock-, and TCR-D115/PD-1:28[tm]-transduced T cells were cocultured with chromium-labeled HEK/Tyr or HEK/Tyr/PD-L1 cells at effector-to-target cell ratio of 6:1 for 4 hours (mean of $n = 2$ experiments + SD). Two-way ANOVA, *, $P < 0.05$. **C,** Increase of IFNγ in cocultures of TCR-D115/PD-1:28[tm]-transgenic T cells with melanoma cell lines relative to D115/MOCK T cells without PD-1:28[tm]. Representative PD-L1 histograms of two melanoma cell lines are shown, isotype (gray filled) and PD-L1 (black line). Numbers are delta mean FI (MFI). **D,** Number of T cells and apoptotic tumor cells observed in 3D SK-Mel23 spheroids 24 hours after exposure to TCR-T58/Mock T cells, TCR-D115/Mock-, or TCR-D115/PD-1:28[tm]–transduced T cells quantified by image analysis. Each symbol represents one spheroid. Histogram overlay shows PD-L1 expression on SK-Mel23 in monolayer culture (solid line), 3D spheroid (dotted line), and isotype staining (gray filled). **E,** Increase of IFNγ in cocultures of TCR53/PD-1:28[tm]-transgenic T cells with nonmelanoma cell lines relative to TCR53/Mock T cells without PD-1:28[tm]. Representative PD-L1 histograms of two RCC cell lines are shown.

Schlenker et al.
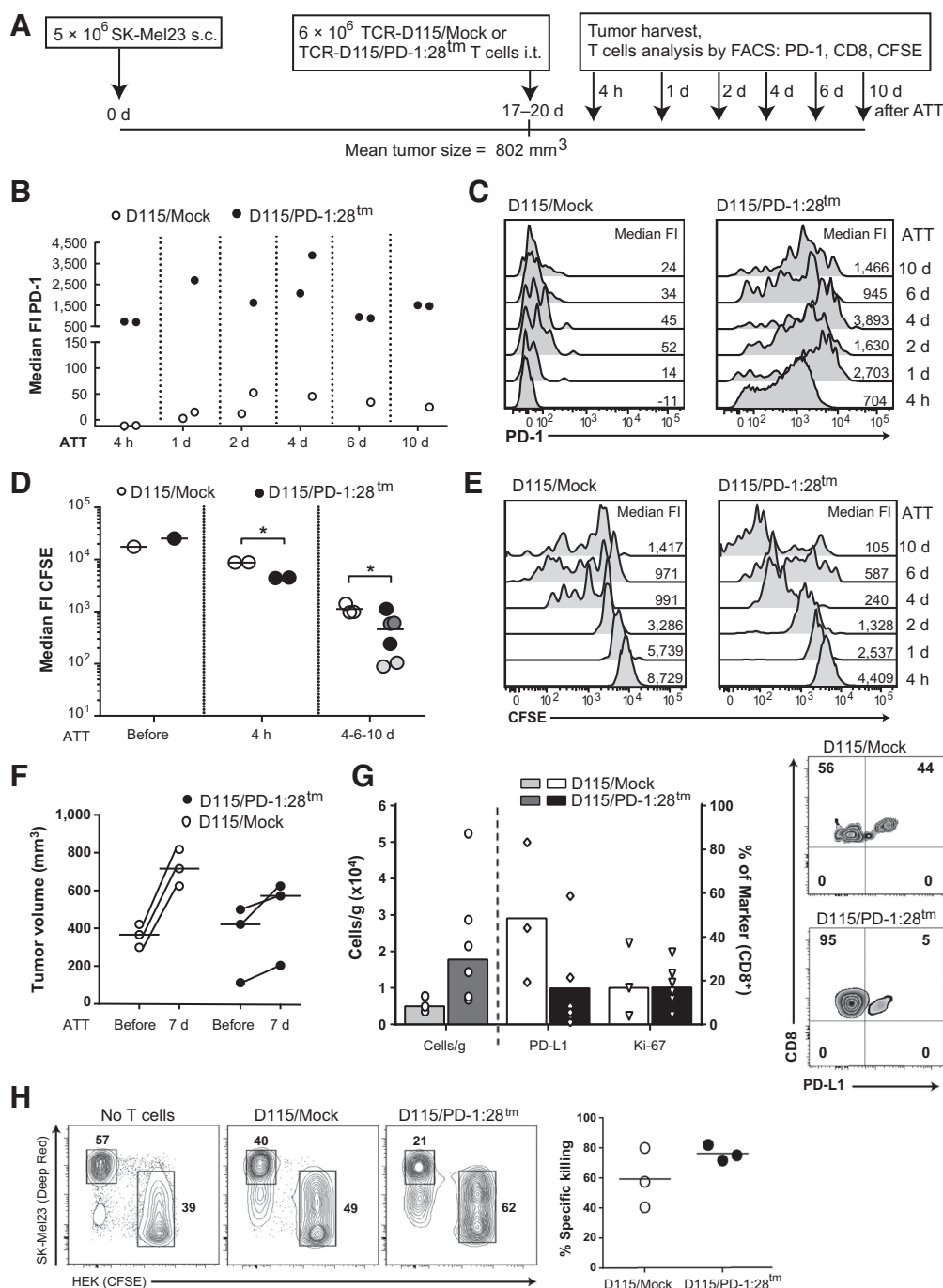
Figure 6.
PD-1:28[tm] fosters intratumoral T-cell proliferation and enables better tumor control in a human melanoma xenograft model. **A,** Outline: 5×10^6 SK-Mel23 (without IFNγ pretreatment) were injected subcutaneously into NSG mice. When tumors reached 802 mm³ ± 83, 6×10^6 CFSE-labeled TCR-D115/Mock or TCR-D115/PD-1:28[tm] T cells were injected intratumorally (transduction efficacy was 88% for TCR-D115 and 76% for PD-1:28[tm]). Tumors were harvested after 4 hours and at 1, 2, 4, 6, and 10 days after ATT. Single-cell suspensions were prepared for flow cytometry. **B** and **C,** Median FI of PD-1 (**B**) and representative PD-1 histograms (**C**) of TILs, gated on CD45+CD8+live leukocytes. **D,** Graph summarizing proliferation (CFSE, median FI) of intratumoral CD45+CD8+TCR-D115/Mock and TCR-D115/PD-1:28[tm] T cells harvested at indicated time points after intratumoral injection. White symbols correspond to TCR-D115/Mock T cells, gray/black symbols to TCR-D115/PD-1:28[tm] T cells. Light gray symbols, 10-day time point; dark gray symbols, 6-day time point; and black symbols, 4-day time point. Sidak multiple comparisons test, *, $P < 0.05$. **E,** Representative histograms showing CFSE staining intensity of CD45+CD8+TCR-D115/Mock and TCR-D115/PD-1:28[tm] T cells in tumor suspensions prepared at indicated time points after intratumoral injection. **F,** Tumor volume before and 7 days after intratumoral T-cell injection. Symbols connected by lines indicate the same mouse; horizontal lines are the median of a group. **G,** Intratumorally injected T cells retrieved from tumors at day 7 and analyzed by flow cytometry. Absolute T-cell counts/g (left axis), percentages of PD-L1 and Ki-67+ T cells (right axis) were determined among gated CD45+CD8+ live lymphocytes. Bars represent the median of a group, and each symbol corresponds to one mouse. Representative dot plots of PD-L1 expression on gated CD8+ T cells. **H,** In situ killing using Matrigel plug assay. Representative dot plots of SK-Mel23/HEK293 mixtures without T cells, with TCR-D115/Mock or TCR-D115/PD-1:28[tm] T cells gated on live/CD45−/PKH26+ cells and graphical summary (each symbol represents one mouse; horizontal line indicates mean of the group).
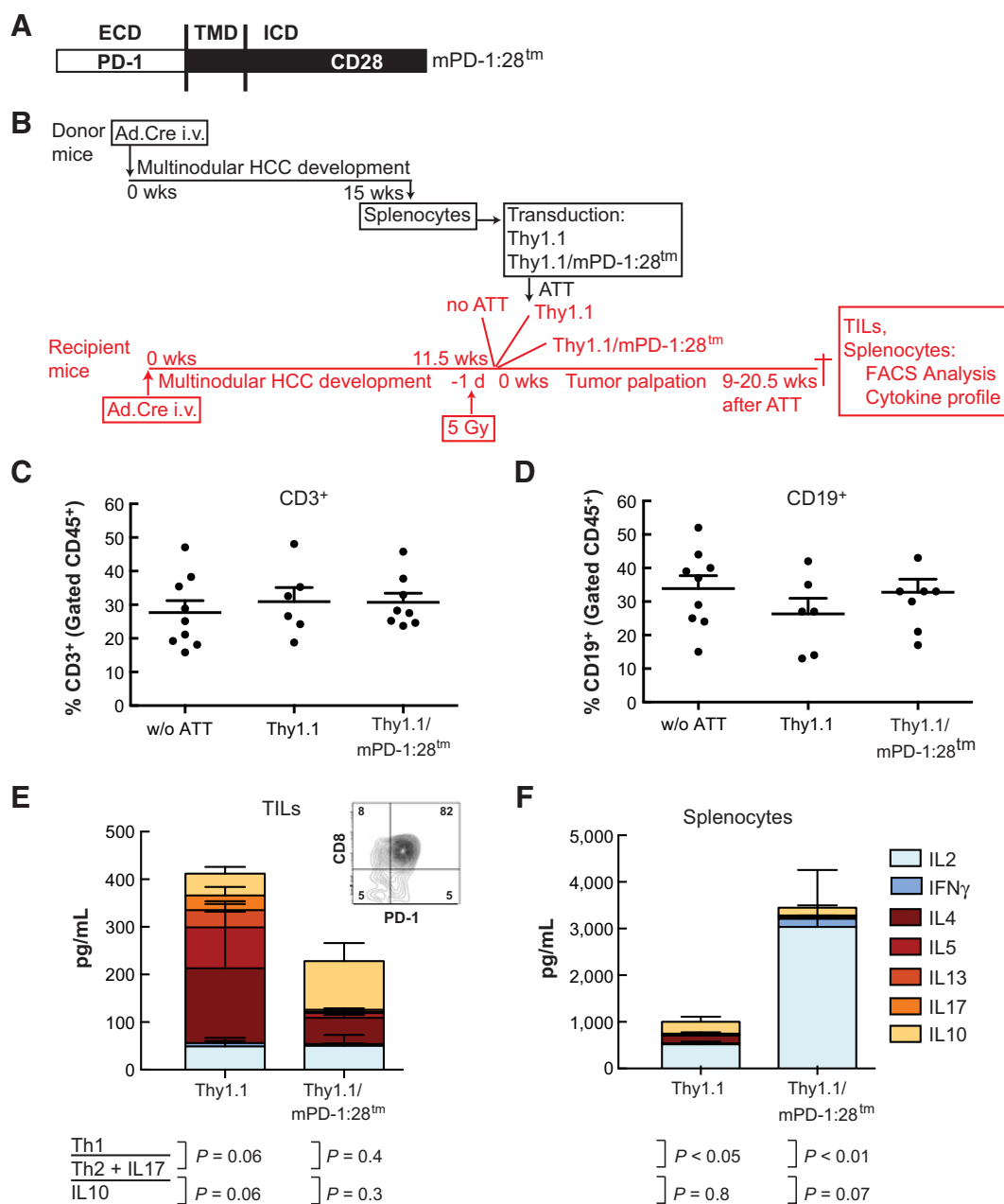
Figure 7.
ATT with mPD-1:28[tm]-positive T cells shifts the cytokine balance in favor of antitumoral Th1 cytokines in an autochthonous HCC model. **A,** Design of the murine PD-1:28[tm] receptor. White regions, domains derived from PD-1; black regions, CD28-derived domains. **B,** Outline of ATT. Donor mice: Splenocytes were isolated from mice 15 weeks after Ad.Cre injection and transduced with Thy1.1 or Thy1.1 together with mPD-1:28[tm]. Recipient mice are mice that had been injected with Ad.Cre 11.5 weeks earlier. Mice were irradiated with 5 Gy one day prior to ATT and received either no ATT or 5×10^6 of Thy1.1 or Thy1.1/mPD-1:28[tm] T cells (retro-orbital injection). Mice were sacrificed when tumors reached a size approximately 1.5 cm, and spleens as well as tumors were harvested for T-cell analysis. **C** and **D,** Scatter dot blots showing % CD3^{+} cells (**C**) and % CD19^{+} cells (**D**) among gated CD45^{+} live cells within tumor suspensions (TIL; mean + SEM) of untreated mice (w/o ATT) and mice treated with Thy1.1 or Thy1.1/mPD-1:28[tm] T cells. **E** and **F,** TILs and splenocytes of mice treated with Thy1.1 or Thy1.1/mPD-1:28[tm] T cells were stimulated with the autologous HCC cell line 434 for 16 hours. Coculture supernatants were analyzed for cytokine content by Bio-Plex (Th1/Th2 panel including IFNγ, IL2, IL4, IL5, IL13, and additionally IL17 and IL10). Stacked bars showing the amount (mean ± SEM) of produced cytokines. Significance between the ratios of Th1 (IL2, IFNγ) to Th2+Th17 (IL4, IL5, IL13, IL17) to IL10 cytokines is shown. Wilcoxon matched-pairs signed rank test. Representative dot plot in **E** shows that CD8-TILs from HCC tumors are highly PD-1^{+}.

(1, 2, 33). Loss of function, exhaustion, and poor persistence of transferred T cells within the tumor microenvironment hinder the efficacy of ATT. T-cell function depends on activation of signaling cascades downstream of the TCR supported by costimulation, which we are able to modify to overcome impediments of ATT. Costimulation increases the MAP kinase activation required for

cytokine secretion and degranulation and supports TCR-independent programs downstream of AKT/mTOR, such as survival, cell-cycle progress, glucose consumption, and restoration of lytic proteins, which are particularly valuable in a restricting environment (23, 24). Human CD8^{+} T cells lose CD28 costimulatory receptor expression during effector–cell differentiation (34), and epithelial cancers generally do not express cognate ligands CD80 or CD86 (35, 36); thus, T cells are unable to receive proper costimulation in this situation. In the context of ATT, low-avidity T cells may not be sufficiently active for tumor elimination due to low functional responses. Yet, they represent the majority of antitumor-reactive T cells and are relatively resistant to the suppressive tumor environment (13, 37). Harnessing them for the antitumor response would enlarge and enrich the spectrum of T cells for ATT. As previous data have shown that PD-1:28 receptors can improve TCR- and chimeric antigen receptor (CAR)-engineered T cells (25, 26, 38, 39), we engineered low-avidity T cells with a PD-1:28 chimeric signaling receptor to explore whether their functional activity could be enhanced allowing their inclusion in a library of TCRs for ATT.

We show that PD-1:28 chimeric receptor can be stably expressed on the surface of human T cells. Surprisingly, the CD8[tm]-linker destabilized surface expression, although similar sequences are effectively used in expression constructs of CAR receptors. We demonstrate that ligation of PD-1:28 overcomes important hurdles in ATT. PD-1:28 engineering invigorated TILs that were functionally disabled in human RCC environments. These TILs recovered Th1-cytokine secretion without unleashing Th2 or IL10 programs presumably based on restoration of ERK and AKT pathways as shown in our *in vitro* coculture system and previous work using similar receptors (25, 26). PD-1:28 ameliorated T-cell inhibition that involved native PD-1/PD-L1 interactions and induced the costimulatory signaling pathway. The combined effect was stronger on the low-avidity TCR-D115-T cells compared with the high-avidity TCR-T58-T cells. Indeed, PD-1:28 cosignaling upgraded low-avidity TCR-D115-T cells to approximate cytokine and cytotoxic response levels of high-avidity TCR-T58-T cells. Thus, PD-1:28 engineering should allow harnessing the advantages of low-avidity T cells for the antitumor response.

PD-1:28 engineering enhanced the T-cell effector response against melanoma, RCC, squamous cell carcinoma, and glioblastoma cell lines. Response enhancement depended on PD-L1 surface expression level on the tumor cells. Thus, PD-1:28 engineering will deliver benefit in conditions with high PD-L1 expression, that is, in tumor milieus. Further evidence that PD-1:28[tm] engineering can support T cells in a "hostile" tumor microenvironment was provided by a human xenograft model using large SK-Mel23 tumors with established T-cell–inhibitory conditions. Here, as was observed in SK-Mel23 spheroids, PD-1:28[tm]–engineered low-avidity TCR-D115-T cells proliferated significantly more and reached higher absolute cell numbers compared with TCR-D115-T cells without the chimeric receptor. TCR-D115/PD-1:28[tm] T cells also showed higher tumor cell killing. Proliferation and killing are important prerequisites for CD8^{+} T cells to cause tumor shrinkage (19, 40, 41). Tumors injected with low-avidity D115/PD-1:28[tm] T cells grew slower over 7 days than tumors injected with TCR-D115 T cells. In future the xenograft animal experiments will be extended to larger sample sizes with longer observation times based on regulatory authority approval.

To determine the potential effect of PD-1:28[tm] on tumor progression, a murine model of autochthonous HCC was used where tumors develop after activation of the SV40-TAg (28). This tumor model resembles the human situation in its slow course of tumor progression, spanning up to 35 weeks from initiating the oncogenic process until death from tumor load. ATT using T cells engineered with a murine PD-1:28[tm] showed positive effects on T-cell polarization. Most notable was the prevention of Th2 and Th17 cytokine secretion. The reduction of Th2 cytokines may be attributed to PD-1:28[tm] deflecting native Th2-polarizing PD-1/PD-L1 interactions into Th1-favoring costimulatory pathways. Similarly, augmentation of Th1 cytokines was observed in patients treated with PD-1 blockade (41). ATT with PD-1:28[tm]-positive T cells also resulted in more IL10, which may enhance cytotoxicity and IFNγ secretion by CD8^{+} T cells and tumor growth, but may also suppress antitumor immunity (42, 43).

Despite positive effects of PD-1:28[tm] on T-cell performance in ATT, this was not sufficient to change tumor growth characteristics in this murine tumor model. Effects on tumor growth have been documented in a mouse model with subcutaneous tumors overexpressing an artificial antigen (ovalbumin) and PD-L1 (44). In our model with tumor development over an extended time period using native antigen and PD-L1 expression, the tumor immune escape may be more complex (45). Overcoming suppression likely requires additional supportive measurements beyond PD1:28 chimeric receptors, such as inhibition of IL10. This is in line with clinical results of ATT using TILs where benefit was achieved only after patient preconditioning with lymphodepletion and radiation in a multiple TIL injection regimen and coadministration of IL2 (19, 46). We have noted that much higher T-cell numbers can be recovered from xenograft tumors after 7 days when IL15 is administrated intraperitoneally at the day of ATT (data not shown).

In summary, we show that cytokine secretion of functionally disabled human TILs can be restored through a PD-1:28[tm] receptor. PD-1:28[tm] mediated a functional upgrading of low-avidity T cells to the level seen in high-avidity T cells. As a consequence, low-avidity T cells previously considered to be therapeutically inefficient can now be considered for ATT. As the PD-1:28 engineering does not modify the TCR sequence, adverse effects on specificity are not expected, thus making this a safer approach than TCR affinity enhancement (3, 4, 10–12, 47). PD-1:28 chimeric receptors have wider potential applications also for CAR-expressing T cells, where these engineered cells have shown better migration and tumor infiltration (38). Although some benefits on T-cell function and tumor control were observed, more advanced *in vivo* models are needed to better document an improved antitumor response. It may be that the potential impact of PD-1:28 receptors on tumor control cannot be reliably visualized in a murine system (48) as mouse T cells do not lose CD28 (34, 49) and, therefore, may not share the same necessity of facilitated costimulation with human T cells. Moreover, mouse models often fail to correctly predict clinical efficacy. New models, such as advanced tumor spheroid 3D cultures, may be helpful in this regard.

Checkpoint inhibition therapies using PD-1/PD-L1 antibodies may benefit from a combination with PD-1:28–engineered T-cell therapy as therapeutically applied anti-PD-L1/anti-PD-1 antibodies may not reach saturation of all target molecules (50). The supportive effects of PD-1:28 engineering imparted on T-cell function make it an attractive tool for ATT.

Disclosure of Potential Conflicts of Interest

Authors' Contributions

Acknowledgments

Grant Support

References

1. Rosenberg SA, Restifo NP. Adoptive cell transfer as personalized immunotherapy for human cancer. Science 2015;348:62–8.
2. Sharma P, Allison JP. The future of immune checkpoint therapy. Science 2015;348:56–61.
3. Hurwitz AA, Cuss SM, Stagliano KE, Zhu Z. T cell avidity and tumor immunity: problems and solutions. Cancer Microenviron 2014;7:1–9.
4. Hebeisen M, Oberle SG, Presotto D, Speiser DE, Zehn D, Rufer N. Molecular insights for optimizing T cell receptor specificity against cancer. Front Immunol 2013;4:154–64.
5. Janicki CN, Jenkinson SR, Williams NA, Morgan DJ. Loss of CTL function among high-avidity tumor-specific CD8+ T cells following tumor infiltration. Cancer Res 2008;68:2993–3000.
6. Bai A, Higham E, Eisen HN, Wittrup KD, Chen J. Rapid tolerization of virus-activated tumor-specific CD8+ T cells in prostate tumors of TRAMP mice. Proc Natl Acad Sci U S A 2008;105:13003–8.
7. Bendle GM, Holler A, Pang LK, Hsu S, Krampera M, Simpson E, et al. Induction of unresponsiveness limits tumor protection by adoptively transferred MDM2-specific cytotoxic T lymphocytes. Cancer Res 2004; 64:8052–6.
8. Anderson MJ, Shafer-Weaver K, Greenberg NM, Hurwitz AA. Tolerization of tumor-specific T cells despite efficient initial priming in a primary murine model of prostate cancer. J Immunol 2007;178:1268–76.
9. Wilde S, Sommermeyer D, Frankenberger B, Schiemann M, Milosevic S, Spranger S, et al. Dendritic cells pulsed with RNA encoding allogeneic MHC and antigen induce T cells with superior antitumor activity and higher TCR functional avidity. Blood 2009;114:2131–9.
10. Chinnasamy N, Wargo JA, Yu Z, Rao M, Frankel TL, Riley JP, et al. A TCR targeting the HLA-A*0201-restricted epitope of MAGE-A3 recognizes multiple epitopes of the MAGE-A antigen superfamily in several types of cancer. J Immunol 2011;186:685–96.
11. Morgan RA, Chinnasamy N, Abate-Daga D, Gros A, Robbins PF, Zheng Z, et al. Cancer regression and neurological toxicity following anti-MAGE-A3 TCR gene therapy. J Immunother 2013;36:133–51.
12. Linette GP, Stadtmauer EA, Maus MV, Rapoport AP, Levine BL, Emery L, et al. Cardiovascular toxicity and titin cross-reactivity of affinity-enhanced T cells in myeloma and melanoma. Blood 2013;122:863–71.
13. Zhu Z, Singh V, Watkins SK, Bronte V, Shoe JL, Feigenbaum L, et al. High-avidity T cells are preferentially tolerized in the tumor microenvironment. Cancer Res 2013;73:595–604.
14. Jenkins MR, La Gruta NL, Doherty PC, Trapani JA, Turner SJ, Waterhouse NJ. Visualizing CTL activity for different CD8Þ effector T cells supports the idea that lower TCR/epitope avidity may be advantageous for target cell killing. Cell Death Differ 2009;16:537–42.
15. Frey AB, Monu N. Signaling defects in antitumor T cells. Immunol Rev 2008;222:192–205.
16. Prinz PU, Mendler AN, Masouris I, Durner L, Oberneder R, Noessner E. High DGK-alpha and disabled MAPK pathways cause dysfunction of human tumor-infiltrating CD8+ T cells that is reversible by pharmacologic intervention. J Immunol 2012;188:5990–6000.
17. Mendler AN, Hu B, Prinz PU, Kreutz M, Gottfried E, Noessner E. Tumor lactic acidosis suppresses CTL function by inhibition of p38 and JNK/c-Jun activation. Int J Cancer 2012;131:633–40.
18. Igney FH, Krammer PH. Immune escape of tumors: apoptosis resistance and tumor counterattack. J Leukoc Biol 2002;71:907–20.
19. Yee C, Thompson JA, Byrd D, Riddell SR, Roche P, Celis E, et al. Adoptive T cell therapy using antigen-specific CD8+ T cell clones for the treatment of patients with metastatic melanoma: in vivo persistence, migration, and antitumor effect of transferred T cells. Proc Natl Acad Sci U S A 2002;99:16168–73.
20. Lauerova L, Dusek L, Simickova M, Kocák I, Vagundová M, Zaloudík J, et al. Malignant melanoma associates with Th1/Th2 imbalance that coincides with disease progression and immunotherapy response. Neoplasma 2002;49:159–66.
21. Zhang Q, Qin J, Zhong L, Gong L, Zhang B, Zhang Y, et al. CCL5-mediated Th2 immune polarization promotes metastasis in luminal breast cancer. Cancer Res 2015;75:4312–21.
22. Chen L, Flies DB. Molecular mechanisms of T cell co-stimulation and co-inhibition. Nat Rev Immunol 2013;13:227–42.
23. Maric M, Zheng P, Sarma S, Guo Y, Liu Y. Maturation of cytotoxic T lymphocytes against a B7-transfected Nnonmetastatic tumor: a critical role for costimulation by B7 on both tumor and host antigen-presenting cells. Cancer Res 1998;58:3376–84.
24. Krummel MF, Heath WR, Allison J. Differential coupling of second signals for cytotoxicity and proliferation in CD8+ T cell effectors: amplification of the lytic potential by B7. J Immunol 1999;63:2999–3006.
25. Ankri C, Shamalov K, Horovitz-Fried M, Mauer S, Cohen CJ. Human T cells engineered to express a programmed death 1/28 costimulatory retargeting molecule display enhanced antitumor activity. J Immunol 2013;191: 4121–9.
26. Prosser ME, Brown CE, Shami AF, Forman SJ, Jensen MC. Tumor PD-L1 co-stimulates primary human CD8(+) cytotoxic T cells modified to express a PD1:CD28 chimeric receptor. Mol Immunol 2012;51:263–72.
27. Leisegang M, Turqueti-Neves A, Engels B, Blankenstein T, Schendel DJ, Uckert W, et al. T-cell receptor gene-modified T cells with shared renal cell carcinoma specificity for adoptive T-cell therapy. Clin Cancer Res 2010;16:2333–43.

Schlenker et al.

28. Willimsky G, Schmidt K, Loddenkemper C, Gellermann J, Blankenstein T. Virus-induced hepatocellular carcinomas cause antigen-specific local tolerance. J Clin Invest 2013;123:1032–43.

29. Leisegang M, Engels B, Meyerhuber P, Kieback E, Sommermeyer D, Xue SA. Enhanced functionality of T cell receptor-redirected T cells is defined by the transgene cassette. J Mol Med 2008;86:573–83.

30. Pauken KE, Wherry EJ. Overcoming T cell exhaustion in infection and cancer. Trends Immunol 2015;36:265–76.

31. Butte MJ, Keir ME, Phamduy TB, Freeman GJ, Sharpe AH. PD-L1 interacts specifically with B7-1 to inhibit T cell proliferation. Immunity 2007;27: 111–22.

32. Li J, Jie HB, Lei Y, Gildener-Leapman N, Trivedi S, Green T, et al. PD-1/SHP-2 inhibits Tc1/Th1 phenotypic responses and the activation of T cells in the tumor microenvironment. Cancer Res 2015;75:508–18.

33. Khalil DN, Smith EL, Brentjens RJ, Wolchok JD. The future of cancer treatment: immunomodulation. CARs and combination immunotherapy. Nat Rev Clin Oncol 2016;13:394–422.

34. Weng NP, Akbar AN, Goronzy J. CD28(-) T cells: their role in the age associated decline of immune function. Trends Immunol 2009;30: 306–12.

35. Chong H, Hutchinson G, Hart IR, Vile RG. Expression of co-stimulatory molecules by tumor cells decreases tumorigenicity but may also reduce systemic antitumor immunity. Hum Gene Ther 1996;7:1771–9.

36. Tirapu I, Huarte E, Guiducci C, Arina A, Zaratiegui M, Murillo O, et al. Low surface expression of B7-1 (CD80) is an immunoescape mechanism of colon carcinoma. Cancer Res 2006;66:2442–50.

37. Mallone R, Kochik SA, Reijonen H, Carson B, Ziegler SF, Kwok WWNepom GT Functional avidity directs T-cell fate in autoreactive CD4+ T cells. Blood 2005;106:2798–805.

38. Liu X, Ranganathan R, Jiang S, Fang C, Sun J, Kim S, et al. A chimeric switch-receptor targeting PD1 augments the efficacy of second-generation CAR T cells in advanced solid tumors. Cancer Res 2016;76:1578–90.

39. Kobold S, Grassmann S, Chaloupka M, Lampert C, Wenk S, Fabian F, et al. Impact of a new fusion receptor on PD-1–mediated immunosuppression in adoptive T cell therapy. J Natl Cancer Inst 2015;107:107–17.

40. Ribas A, Shin DS, Zaretsky J, Frederiksen J, Cornish A, Avramis E, et al. PD-1 blockade expands intratumoral memory T cells. Cancer Immunol Res 2016;4:194–203.

41. Kalos M, June CH. Adoptive T cell transfer for cancer immunotherapy in the era of synthetic biology. Immunity 2013;39:49–60.

42. Dulos J, Carven GJ, van Boxtel SJ, Evers S, Driessen-Engels LJ, Hobo W, et al. PD-1 blockade augments Th1 and Th17 and suppresses Th2 responses in peripheral blood from patients with prostate and advanced melanoma cancer. J Immunother 2012;35:169–78.

43. Mocellin S, Marincola FM, Young HA. Interleukin-10 and the immune response against cancer: a counterpoint. J Leukoc Biol 2005;78:1043–51.

44. Mumm JB, Emmerich J, Zhang X, Chan I, Wu L, Mauze S, et al. IL-10 elicits IFNgamma-dependent tumor immune surveillance. Cancer Cell 2011; 20:781–96.

45. Chen DS, Mellman I. Oncology meets immunology: the cancer-immunity cycle. Immunity 2013;39:1–10.

46. Rosenberg SA, Dudley ME. Adoptive cell therapy for the treatment of patients with metastatic melanoma. Curr Opin Immunol 2009;21:233–40.

47. Johnson LA, Morgan RA, Dudley ME, Cassard L, Yang JC, Hughes MS, et al. Gene therapy with human and mouse T-cell receptors mediates cancer regression and targets normal tissues expressing cognate antigen. Blood 2009;114:535–46.

48. Mestas J, Hughes CC. Of mice and not men: differences between mouse and human immunology. J Immunol 2004;172:2731–8.

49. Riley JL, June CH. The CD28 family: a T-cell rheostat for therapeutic control of T-cell activation. Blood 2005;105:13–21.

50. Hedge PS, Karanikas V, Evers S. The where, the when, and the how of immune monitoring for cancer immunotherapies in the era of checkpoint inhibition. Clin Cancer Res 2016;22:1865–74.

Cancer Research

AACR American Association
for Cancer Research

Chimeric PD-1:28 Receptor Upgrades Low-Avidity T cells and Restores Effector Function of Tumor-Infiltrating Lymphocytes for Adoptive Cell Therapy

Ramona Schlenker, Luis Felipe Olguín-Contreras, Matthias Leisegang, et al.

Updated version	Access the most recent version of this article at: doi:10.1158/0008-5472.CAN-16-1922
Supplementary Material	Access the most recent supplemental material at: http://cancerres.aacrjournals.org/content/suppl/2017/05/20/0008-5472.CAN-16-1922.DC1

Cited articles	This article cites 50 articles, 27 of which you can access for free at: http://cancerres.aacrjournals.org/content/77/13/3577.full#ref-list-1

E-mail alerts	Sign up to receive free email-alerts related to this article or journal.
Reprints and Subscriptions	To order reprints of this article or to subscribe to the journal, contact the AACR Publications Department at pubs@aacr.org.
Permissions	To request permission to re-use all or part of this article, contact the AACR Publications Department at permissions@aacr.org.